PSEUDODYNAMIC TEST AND FEM ANALYSIS OF RC SHEAR WALLS

Naofumi TERAMOTO[1], Carlos CUADRA[2], Junji OGAWA[3] And Norio INOUE[4]

SUMMARY

To study the seismic behavior and damage patterns of reinforced concrete (RC) shear walls subjected to earthquake motions with different damage potential, pseudodynamic tests using conventional jacks were performed. Nonlinear finite element method (FEM) analysis was also carried out. Two story cantilever type wall specimens, designed to fail in bending, were adopted for the test program. Two identical specimens were constructed and tested under different types of input ground motions. The input motions were generated artificially to have characteristics of short time duration. The long and short duration earthquake motions were generated to be compatible to the same elastic target spectrum and different phase contents. The dynamic model considered had one horizontal degree of freedom and the mass was assumed to be located at the loading point at the top. The specimens were loaded successively from elastic range to large deformation range. The characteristic results such as load-displacement relationships and maximum response displacements of each step were observed. The results of the test were compared computation based on 2D-nonlinear FEM model.

The FEM model was based on smeared models of concrete and reinforcement, and represented by assembling iso-parametric plane elements with 4-nodes. The concrete model considered tension stiffening, and degradation of stiffness and strength after cracking. Reinforcement was modeled by a bi-linear relationship.

From the results, it was found that the specimen subjected to the earthquake motion with long time duration suffered more severe damage than the specimen with short time duration earthquake in inelastic range even if the two earthquake motions had the same elastic response spectrum.

INTRODUCTION

Earthquake motion changes its characteristics depending on the seismic scale, the hypocentral distance and the soil conditions. The response spectra have been widely applied to elucidate the seismic structural damage and also to define the standard level of the seismic scale. However, even if the characteristics of elastic response spectra are the same, the structural damages and inelastic responses are not necessarily the same since loading pattern is different depending on the duration time, such as short duration pulse wave and long duration continuous wave. In this research, pseudodynamic tests and nonlinear finite element method (FEM) analysis were performed on two-story reinforced concrete shear wall specimens by using two duration patterns of waves (short and long).

In the pseudodynamic method, the numerical techniques used in dynamic analysis of structures are combined with the experimental procedures of conventional static tests to evaluate the performance of structures subjected to earthquake loads. The applied nonlinear FEM model was represented by assembling iso-parametric plane elements with 4-nodes. In this study, the dependence of the maximum response displacement on the duration of input motion and loading pattern was investigated, and the results of the experimental were compared with the results of 2-D FEM analysis.

[1] *Dept. of Arch. and Environment Systems, Akita Prefectural University, Honjo, Akita, Japan Email:tera@akita-pu.ac.jp*
[2] *Dept. of Arch. and Environment Systems, Akita Prefectural University, Honjo, Akita, Japan Email:tera@akita-pu.ac.jp*
[3] *Dept. of Arch. and Environment Systems, Akita Prefectural University, Honjo, Akita, Japan Email:tera@akita-pu.ac.jp*
[4] *Dept of Arch. and Building Science, Tohoku University, Sendai, Miyagi, Japan Email: inoue@struct.archi.tohoku.ac.jp*

TEST CONDITIONS

2.1 Specimens

Two specimens with the same scale and the same material characteristics were prepared. The dimension of the specimen and the material characteristics are shown in Table 1 and Table 2, respectively. The general characteristics of these specimens are shown in Figure 1(a). The specimen was a two-story cantilever type wall with an intermediate beam. The bending yield strength of the specimen was 90 kN. The nominal strength of the concrete was 30MPa and the yielding strength of the main reinforcement was 377MPa.

Table 1: Characteristic of Specimens

	Section (mm)	Main reinforcement (ratio, %)	Transverse reinforcement (ratio, %)	
Column	150 x 120	6-D10 (2.3%)	D4@40	(0.4%)
Beam	150 x 120	4-D10 (1.6%)	D4@40	(0.4%)
Wall	Thickness 60	Vertical	Horizontal	
		D4@40	D4@40	

Table 2: Material Properties of Specimens

Nominal concrete strength (MPa)	Steel strength (MPa)	
	D10	D4
30	377	223

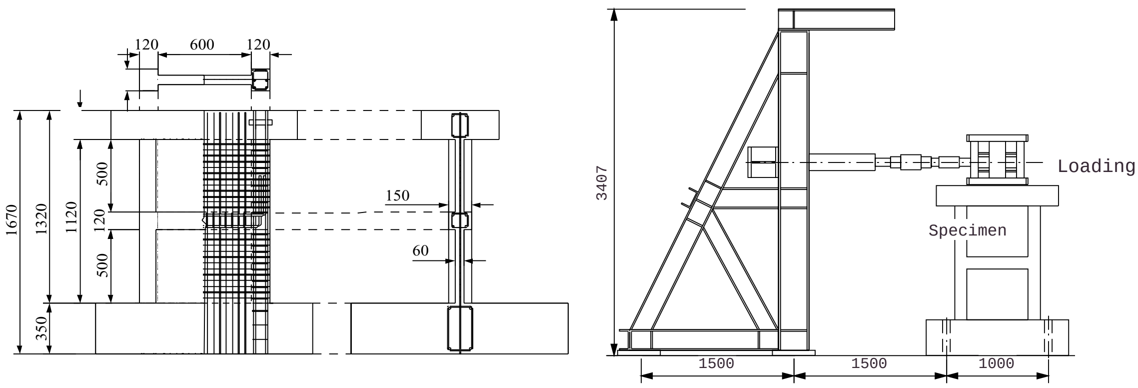

(a) (b)

Figure 1: Specimen and Test Setup

2.2 Experimental Method

The general outline of the test setup is shown in Figure 1(b). The main loading was applied by a reversible-load hydraulic jack (490kN) in the horizontal direction and in the plane of the wall. To prevent the displacement of the specimen in the direction perpendicular to the main loading, another jack was set in this direction. The loading height measured from the base top to the horizontal axis of the loading jack was 1550mm. Axial load was not applied in this test.

2.3 Pseudodynamic System

The numerical algorithm for analysis and the experimental system reported by Cuadra et al. (Cuadra, Inoue and Ogawa,1998) were used in this study. The system was modeled as a one degree of freedom system and the Newmark-β (β=0) method for numerical integration was used to solve the dynamic equation of motion. The applied numerical formula of the test is shown in Eq.(1) and the flow chart of the integration scheme is shown in Figure 2.

$$
\begin{aligned}
d_{i+1} &= d_i + \Delta t v_i + \frac{\Delta t}{2} a_i \\
a_{i+1} &= \left(m + \frac{\Delta t}{2} c \right)^{-1} \left[f_{i+1} - r_{i+1} - \frac{\Delta t}{2} c a_i \right] \qquad (1) \\
v_{i+1} &= v_i + \frac{\Delta t}{2} \left(a_i + a_{i+1} \right)
\end{aligned}
$$

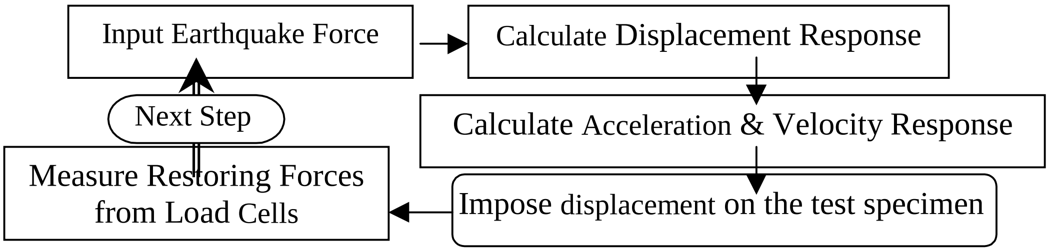

Figure 2: Flow Cart of the Integration Scheme

Here r_i, a_i, v_i and d_i, respectively, are restoring force, response acceleration, velocity and displacement on i step and m, c are mass and damping, respectively. The mass was assumed to be 2.0MN so that the initial period of the system might be approximately 0.3 second. The viscous damping was assumed as zero. During the test, two computers were used for the main control of the testing process and for data acquisition, respectively.

2.4 Input Motion

Two input motion with long time duration wave (Case L) and short time duration wave (Case S) were used to examine the effects of the time duration on the response behavior and on the structural damage. These two waves were simulated seismic waves with the same response acceleration spectrum and different phase content and different time duration. Case L, input motion had the phase content obtained from the earthquake motion recorded at Tohoku University NS (1978 Off Miyagi Prefecture) that corresponds to a far-source type input motion. In Case S the phase content corresponds to the record obtained at Sylmar County Hospital NS (1994 Northridge) which represents a near-source input motion. In both cases the input motions were modified to match the same target spectrum that is shown in Figure 3. The modified waves are shown in Figure 4. The time duration for Case L was 20s and that for Case S 10s. The target spectrum was 50 gal flat within the target period of the specimen. As shown in Table 3, input level was varied at four steps from elastic level to plastic level (Run 1 - Run 4) by multiplying the waves by appropriate coefficients.

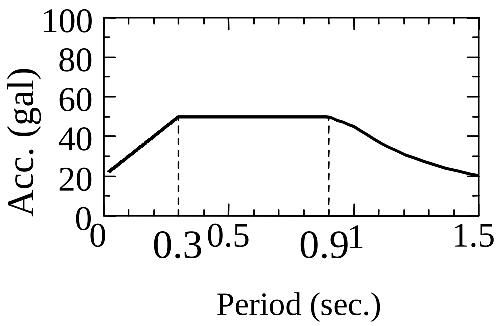

Figure 3: Target Spectrum

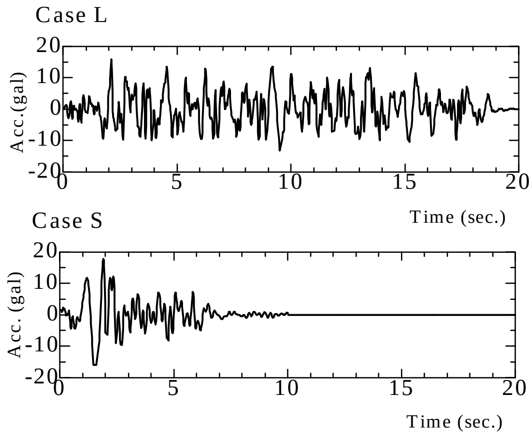

Figure 4: Simulated Input Motions

Table 3: Input level

	Target level	Input ratio
RUN1	Elastic range	x 0.7
RUN2	Inelastic range	x 1.1
RUN3		x 1.3
RUN4	Plastic range (after yield of reinforcement)	x 2.0

3. EXPERIMENTAL RESULTS

Figures 5 and 6 show the response displacement and load-displacement relationship, respectively. The bending yield occurred in RUN2 for Case L, and in RUN3 for Case S. Many peak displacements of the order of the maximum displacements were observed for Case L, while for Case S large displacements, including the maximum displacements, were observed within a short time. This is due to the difference in the characteristics of each input motion. In RUN1 - 3 for Case S, the response displacements in the both senses (positive and negative) were large. On the other hand, in Run 4 for Case S, only the positive displacement was large. The maximum values of the response displacement, velocity and acceleration are shown in Table 4. The larger value between the responses observed in Case L and Case S at each run is underlined. It should be noted that except for Run 4, the maximum displacements for Case L were larger than those for Case S. Only in RUN4, the maximum response displacement for Case S was larger than that for Case L. The main reason for this is probably that the response spectrum obtained from the input motion for Case L became smaller than the target spectrum at about the period of the specimen for RUN4 (Teramoto, Inoue, Ogawa and Hoshi,1999).

Table 4: Maximum Values of Response

	Maximum response displacement (mm , [rad.])		Maximum response velocity (cm/s)		Maximum response acceleration (gal)	
	Case L	Case S	Case L	Case S	Case L	Case S
RUN1	**2.4 [1.9x10^{-3} rad]**	1.4 [1.19x10^{-3} rad]	2.50	1.77	32.3	25.5
RUN2	**5.0 [4.1 x10^{-3} rad]**	3.6 [2.99x10^{-3} rad]	4.23	3.40	47.8	47.3
RUN3	**7.2 [5.9 x10^{-3} rad]**	5.6 [4.69x10^{-3} rad]	5.25	4.50	50.4	56.5
RUN4	13.6[11.2 x10^{-3} rad]	**15.3[12.7x10^{-3} rad]**	8.07	7.95	57.2	62.7

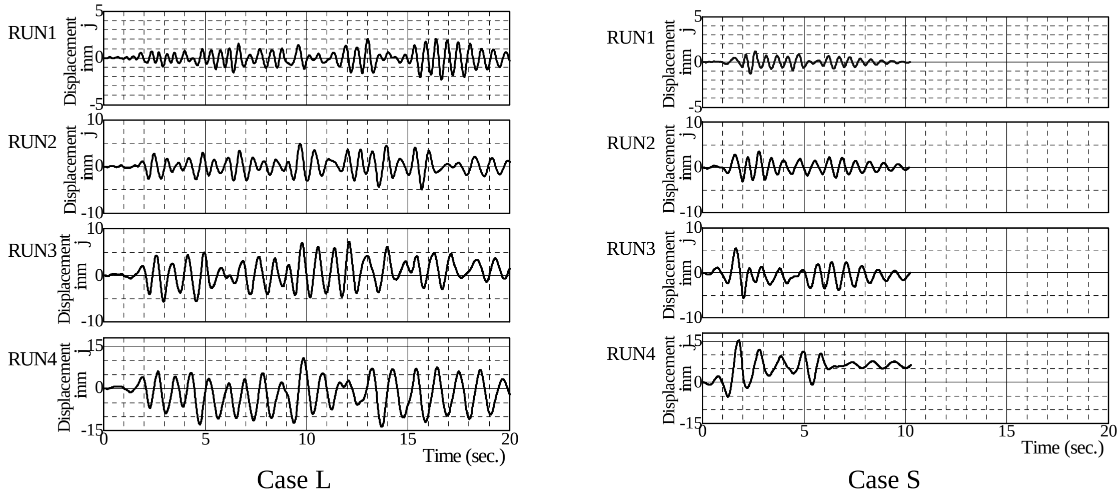

Figure 5: Response Displacement

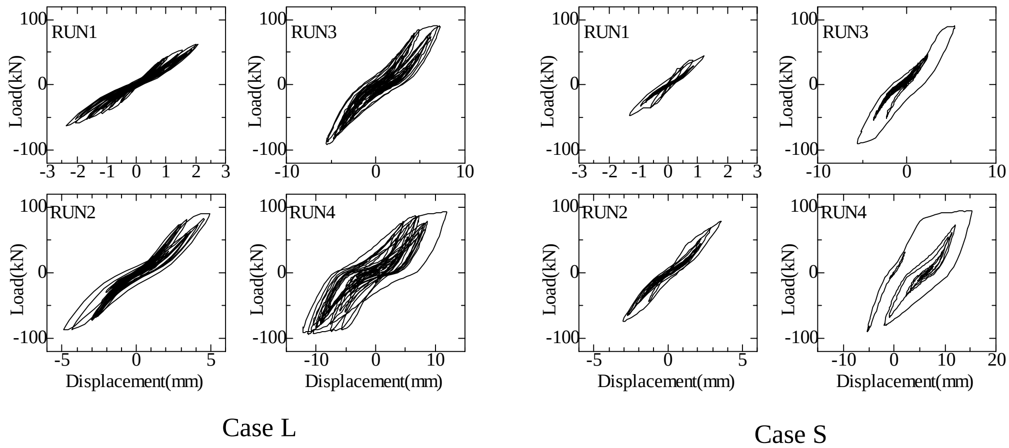

Figure 6: Load-Displacement Relationship

4.FEM MODEL

The applied FEM model consisted of plane model for wall, column and beam, and joint model for the critical cross section. The plane model was based on smeared models of concrete and reinforcement, and represented by assembling iso-parametric plane elements with 4-nodes. Considering that the bond slip between steel bars and surrounding concrete seemed to be observed at the joint above the base of the specimen in the test, the joint model was applied at the bottom of the specimen. The FEM model of the specimen is shown in Figure 7.

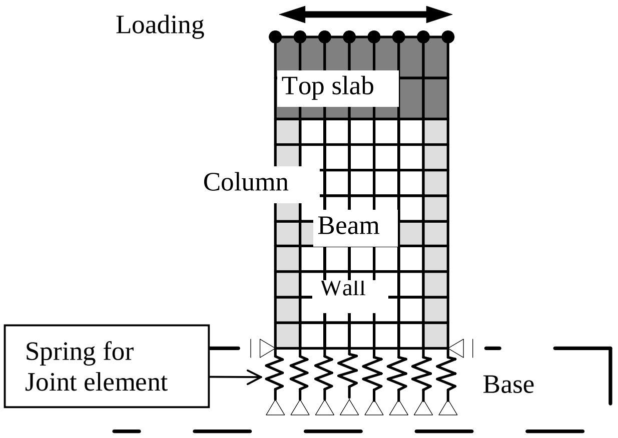

Figure 7: FEM model of the specimen

4.1 Plane Elements

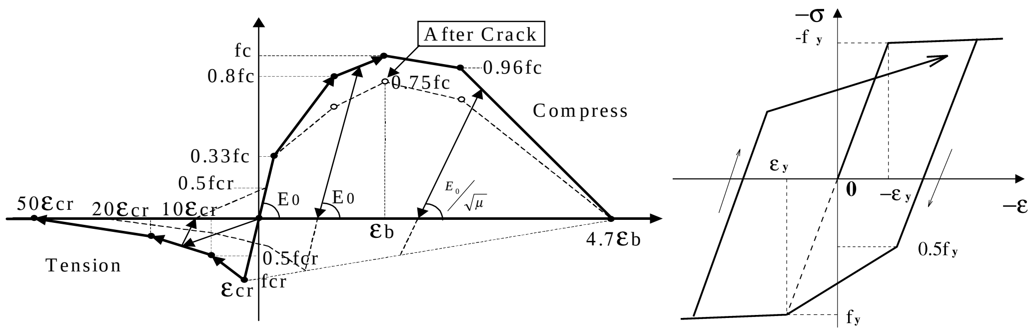

(a) concrete (b) reinforcement

Figure 8: Stress-strain relationships of plane elements

The stress-strain relationships of the concrete and reinforcement are shown in Figs. 8(a) and (b), respectively. The concrete model considered tension stiffening and degradation of stiffness and strength after cracking. This model also considered how the stress-strain relationship in the compression region relates to that in the tension region. Reinforcement was modeled by a bi-linear relationship. The concrete before cracking was assumed to be equivalent isotropic, and material stiffness matrix $[D_C]$ is given by Eq. (2) in the principal coordinates.

$$[D_C] = \frac{E_i}{1-\nu^2}\begin{bmatrix} 1 & \nu & 0 \\ \nu & 1 & 0 \\ 0 & 0 & \frac{1-\nu}{2} \end{bmatrix} \tag{2}$$

Here, ν is the Poisson's ratio and E_i is the tangential modulus given by the assumed stress-strain relationship which is obtained for the larger principal stress. The concrete after cracking was assumed to be the stiffness matrix expressed by Eq. (3).

$$[D_C] = \begin{bmatrix} E_{C1} & 0 & 0 \\ 0 & E_{C2} & 0 \\ 0 & 0 & G_C \end{bmatrix} \tag{3}$$

Here, E_{C1} and E_{C2} are the tangential moduli given by the assumed stress-strain relationship, and G_C is the tangential shear stiffness after cracking.
The degradation ratio of the compression strength of the concrete in the direction perpendicular to the crack was assumed to be a constant value of 0.75.

4.2 Joint Elements

As shown in Fig. 7, joint springs which had degree of freedom only in the vertical direction were placed below the test specimen in order to simulate the bond slip movement of the vertical reinforcement. The joint springs in each element consisted of two springs connected in series. The one spring, which is called here an bond slip spring, was considered to behave as the bond slip of the vertical reinforcement in the base, and the another spring, which is called here a plastic spring, was considered to behave as the plastic region of the reinforcement around the joint section, in which the yield of the reinforcement occurs, of the base and the specimen. The plastic spring was assumed to approximately follow a bi-linear relationship. The stress-displacement relationship of the above mentioned two springs is shown in Fig. 9. Here, F_y expresses the yield strength of the steel. At point 1 in Fig. 9, crack appears in the concrete of the joint section and the bond slip starts. The stress at point 1 was determined from the cross-sectional area of the specimen by assuming the tensile strength to be one tenth of the compression strength of the concrete. The bond slip length when the yield of reinforcement occurs was determined as follows. As shown Fig. 10 (a), the effective transmission length of the reinforcement in the base of specimen (L_d) was determined by assuming uniform distribution of the bond stress along the reinforcement, and then the bond slip length was determined by integrating the strain of reinforcement along the effective transmission length. Here, the strain distribution of reinforcement was assumed as described in Fig. 10 (b).

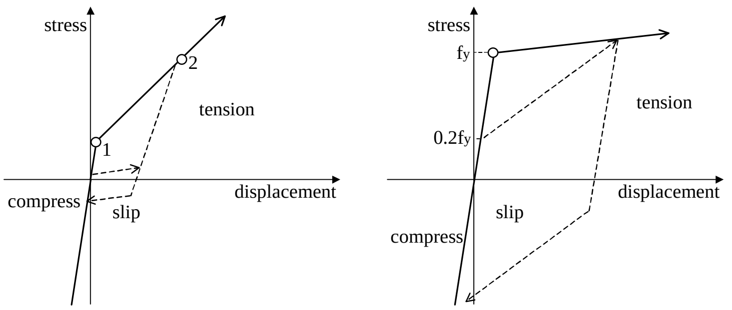

(a) Bond slip spring (b) Plastic spring

Figure 9: Stress-displacement relationship of joint spring

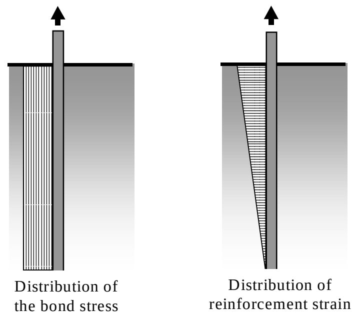

(a) (b)

Figure 10: Bond stress and effective transmission length of steel bar

4.3 Dynamic Analysis Method

In order to realize the situation of the experiment in the analysis, the numerical integration method used in the experiments (Newmark β [β=0]) was also used in the analysis to solve the dynamic motion equation. For this purpose, the test specimen in the FEM model was loaded until the target displacement was attained in the calculation at each step to calculate the restoring force, which was used in determining the target displacement in the subsequent step. The viscous damping was assumed zero. At the beginning of each dynamic analysis, the model specimen was loaded so that $\pm$3mm displacement of the top slab in the horizontal direction might occur statically in order to match the initial period of the specimen in the analysis with that in the pseudodynamic test.

5. COMPARISON OF TEST AND ANALYTICAL RESULTS

Dynamic analysis of the results from RUN1 to RUN4 for both Case L and Case S was performed. The comparison between the analysis and test results of the response displacement and that of the load-displacement relationship are shown in Figs. 11 and 12, respectively. As shown in Fig. 12, the analytically obtained envelope curves agree fairly well with the experimentally observed results. However, the internal hysteresis area obtained in the experiment was smaller than that by the analysis. As shown in Fig. 11 for Case S, the analytically calculated amplitude after the maximum response displacement in each run was smaller than the test result.
The same phenomenon was also observed in Case L, especially in RUN 3 and RUN4. However, in both Case S and Case L, almost the same residual displacements at the end of the experiments were obtained in both the experiments and the calculations. The comparison between the maximum response displacements in Case L and Case S is shown in Table 5. Generally, when the response was small, the analysis gave larger results than the test results. On the other hand, when the response became larger as seen in RUN3 and RUN4, analysis gave smaller results. In the comparison between the maximum values at each run in Case L and case S, the Case L gave larger values except RUN4. This is in agreement with the experimental results.

Table 5: Comparison of maximum response displacement

	Case L		Case S	
	TEST	FEM	TEST	FEM
RUN1	2.4 mm	2.6 mm	1.3 mm	1.6 mm
RUN2	5.0 mm	5.0 mm	3.6 mm	4.5 mm
RUN3	7.2 mm	6.7 mm	5.6 mm	6.1 mm
RUN4	13.6 mm	9.4 mm	15.3 mm	14.9 mm

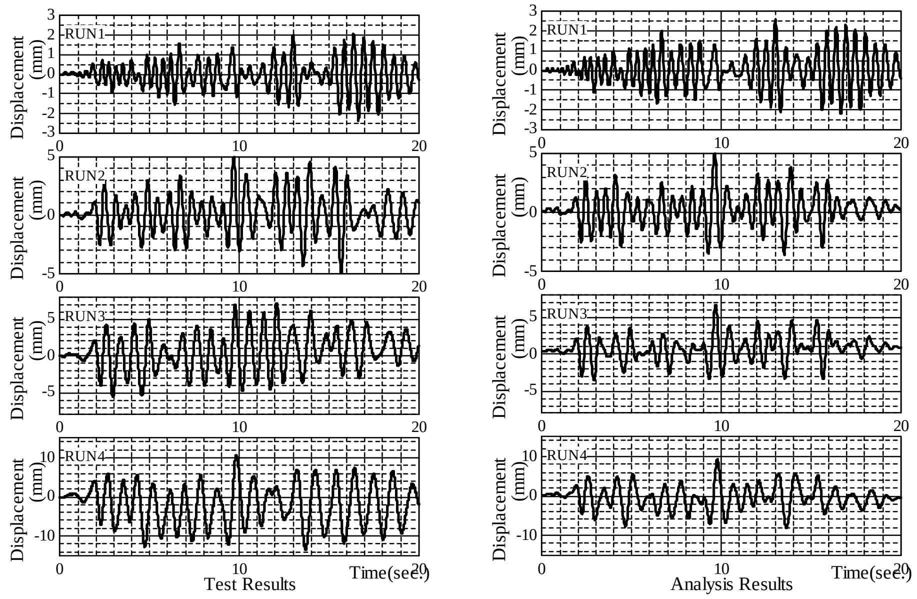

(a) Case L

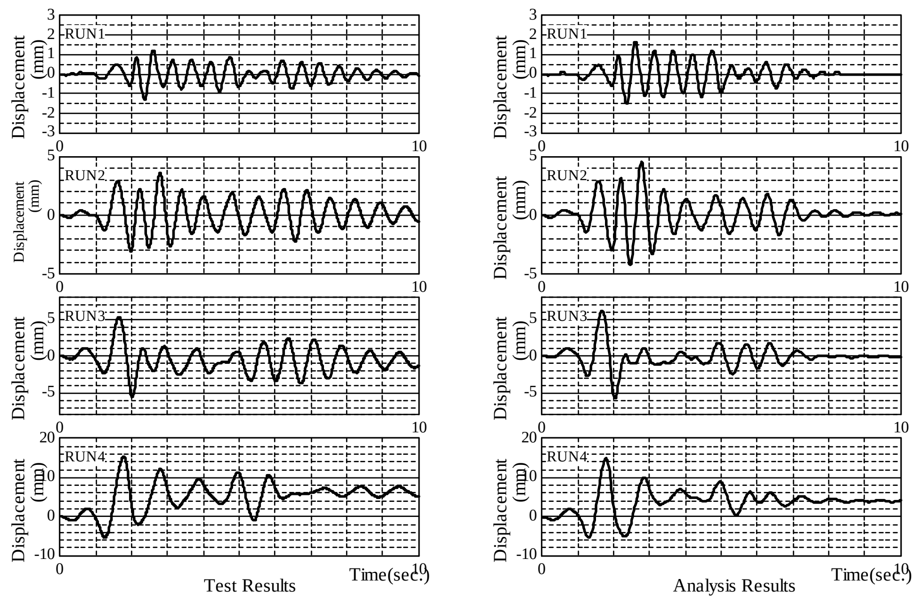

(b) Case S

Figure 11: Time history of response displacement

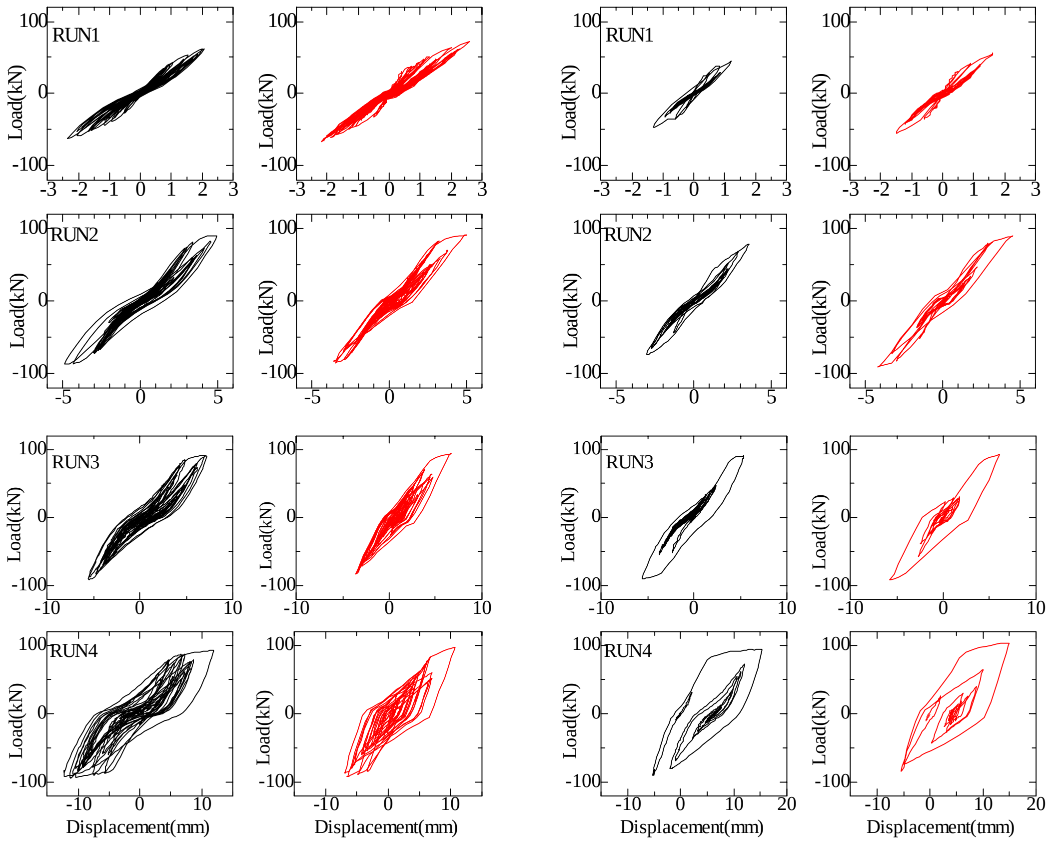

Test results Analysis results Test results Analysis results

(a) Case L (b) Case S

Figure 12: Load-displacement relationship

6. CONCLUSION

A series of pseudodynamic test of the cantilever two-story shear wall specimen was performed using the two input waves with different time duration and with same response spectrum. The two dimensional nonlinear FEM analysis was also performed to simulate the experimental results. The following conclusions were obtained.

(1) Large difference between the load-displacement behavior for long duration earthquake and short duration earthquake was observed. In addition, the load-displacement behavior of for short duration input changed considerably from the initial step to the final step. These test results were successfully simulated by the analysis.

(2) Analytically calculated response was in agreement with experimental results in all cases, particularly around the time when the maximum response displacement occurred.

(3) The tendency of increased maximum response displacement with the increase in the duration of motion was noted.

REFERENCES

Cuadra, C., Inoue, N. and Ogawa, J.(1998), "Pseudodynamic test to study the behavior of reinforced concrete columns subjected to two dimensional input motions", *Proceedings of the Eleventh European Conference on Earthquake Engineering*, Abstract Volume, pp163 (CD-ROM)

Inoue, N., Yang, K. and Shibata, A.(1997),"Dynamic nonlinear analysis of reinforced concrete shear wall by finite element method with explicit analytical procedure", *Earthquake Engineering & Structural Dynamics*, Vol.26, No.9, pp967-986

Okamura, H., Maekawa, K.(1991),"Nonlinear Analysis and Constitutive Models of Reinforced Concrete", *Gihodo* , Japan

Teramoto, N., Inoue, N., Ogawa, J. and Hoshi, M.(1999),"Pseudodynamic test of RC shear walls subjected to earthquake motions with different duration", *Journal of Structural Engineering*, *AIJ*, Vol.45B, pp321-328 (In Japanese)